

## Rapid Communication

# Continuous nanoparticle production by microfluidic-based emulsion, mixing and crystallization

Y.-F. Su\*, H. Kim, S. Kovenklioglu, W.Y. Lee

Department of Chemical, Biomedical and Materials Engineering, New Jersey Center for MicroChemical Systems, Stevens Institute of Technology, Hoboken, NJ 07030, USA

Received 10 April 2007; received in revised form 6 June 2007; accepted 10 June 2007  
Available online 20 July 2007

## Abstract

BaSO<sub>4</sub> and 2,2'-dipyridylamine (DPA) nanoparticles were synthesized as reactive crystallization and anti-solvent recrystallization examples, respectively, of using the microfluidic-based emulsion and mixing approach as a new avenue of continuously producing inorganic and organic nanoparticles. BaSO<sub>4</sub> nanoparticles in the size range of 15–100 nm were reactively precipitated within the confinement of an aqueous droplet which was coalesced from two separate aqueous droplets containing BaCl<sub>2</sub> and (NH<sub>4</sub>)<sub>2</sub>SO<sub>4</sub> using a three T-junction micromixer configuration constructed with commercially available simple tubing and fitting supplies. Also, DPA nanoparticles of about 200 nm were crystallized by combining DPA+ethanol and water droplets using the same micromixer configuration.

© 2007 Elsevier Inc. All rights reserved.

**Keywords:** Nanoparticles; Microfluidics; Microreactor; Emulsion; Crystallization

## 1. Introduction

Microreactors offer many paradigm-changing opportunities for exploring new chemical synthesis routes due to potential for precisely managing heat and mass transfer characteristics at sub-millimeter length scales [1]. More recently, microreactors have been also explored as new laboratory tools for high-speed protein crystallization studies [2] and for continuous colloidal processing [3]. For example, Khan et al. [4] recently reported that silica particles could be synthesized with precise control over size and distribution. Homogenous distribution of reactants and temperatures inside the microchannel and continuous operation at steady-state conditions offer the microreactor technology advantages over conventional batch methods for controlling particle size and distribution [5]. Also, organic nanoparticles have been successfully prepared by various microemulsion methods as Debuigne et al. [6] reported. On another research front, significant advances have been made in the use of microfluidic devices for

controlling the size, size distribution and shape of water-in-oil (W/O) emulsion [7–10]. Conventionally, emulsions are generated by mixing two immiscible fluids [5,11]. The advantage of the microfluidic-based emulsion approach is the ability to control water droplet size and solute compositions within the droplets [5]. In this investigation, we explore an integrative use of microfluidic-based emulsion and mixing of two types of aqueous droplets, with commercially available simple tubing and fitting supplies, for reactive and anti-solvent crystallization as new avenues of continuously producing inorganic and organic nanoparticles.

## 2. Experimental

Fig. 1 shows our experimental apparatus, which basically consisted of three T-junction micromixers. Teflon® tubing with 500 μm ID and Teflon® tees were used to assemble the T-junction micromixers. Two of the micromixers (i.e.,  $T_A$  and  $T_B$  in Fig. 1) were used to produce aqueous solution droplets of A and B in vegetable oil (Wesson, 100% pure corn oil) emulsion. The solution A and solution B droplets were coalesced at the third

\*Corresponding author. Fax: +1 201 216 8306.

E-mail address: [Yi-Feng.Su@stevens.edu](mailto:Yi-Feng.Su@stevens.edu) (Y.-F. Su).

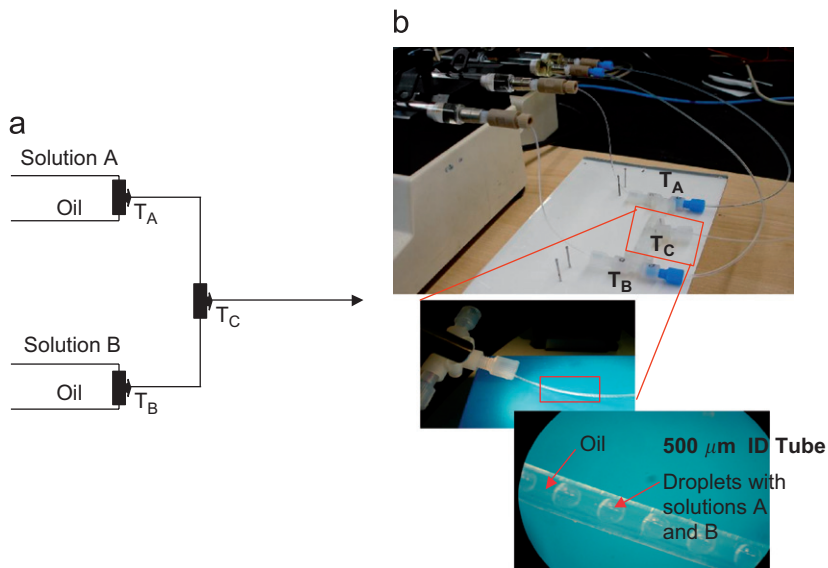
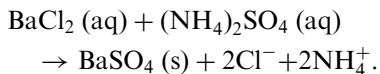


Fig. 1. Experimental apparatus: (a) schematic illustration and (b) photographs of T-junction mixers and close-up picture of water-in-oil droplets.

micromixer ( $T_C$ ). As shown in Fig. 1b, the size of the aqueous droplets was about 500  $\mu\text{m}$ , which corresponded to the inner diameter of the Teflon® tube. Syringe pumps were used to control the flow rates of the A, B and two oil streams at 0.15, 0.15 and 0.25 ml/min, respectively. These flow conditions provided the most optimum conditions for generating stable emulsions and coalescing the A and B droplets at  $T_C$ .

For reactive crystallization, 0.01 M  $\text{BaCl}_2$  and 0.01 M  $(\text{NH}_4)_2\text{SO}_4$  were used as solutions A and B in the first experiment. In the second experiment, the  $\text{BaCl}_2$  concentration was increased to 0.015 M. The solubility values of  $\text{BaCl}_2$  and  $(\text{NH}_4)_2\text{SO}_4$  in water are 0.37 g/g  $\text{H}_2\text{O}$  and 0.76 g/g  $\text{H}_2\text{O}$ , respectively [12]. Upon coalescence of the A and B droplets,  $\text{BaCl}_2$  and  $(\text{NH}_4)_2\text{SO}_4$  reacted to precipitate  $\text{BaSO}_4$ :



$\text{BaSO}_4$  is commercially used as a magnetic resonance imaging agent, is poorly soluble in water (0.31  $\mu\text{g/g}$   $\text{H}_2\text{O}$  at 25 °C) and the rate of the precipitation reaction is known to be very fast [13]. The exit stream was collected in a beaker, and de-ionized water was added to separate the aqueous phase from the oil phase and dilute the aqueous solution.

For comparison,  $\text{BaSO}_4$  particles were also produced in a beaker to compare and contrast the beaker-based W/O emulsion method with the microfluidic-based emulsion method. The same precursor concentrations were used in this experiment, i.e., 0.01 M  $\text{BaCl}_2$  and 0.01 M  $(\text{NH}_4)_2\text{SO}_4$ . The vegetable oil and aqueous solution ratio was 3:1. The resulting particles were then filtered and dried in an oven.

For anti-solvent crystallization, 2,2'-dipyridylamine (DPA, the acid forms of the hydrated salt), was used as a model organic compound. Anti-solvent crystallization has been commonly used to produce various crystals such as

sodium nitrate and sodium chloride [14,15]. In this crystallization method, DPA was first dissolved in a mixture of ethanol and water to nearly its solubility level. DPA is soluble in ethanol, but not in water whereas ethanol and water are completely miscible. This makes water a suitable anti-solvent, as further water addition to the solution lowers the solubility of DPA in the mixture and thus generates the supersaturation, which drives the crystallization process. The solubility considerations for emulsion-based anti-solvent crystallization are important for the viability of this method. We have found that DPA is essentially insoluble in the oil and the solubility of ethanol in the oil is about 10%. A total of 0.0609 g DPA was dissolved in an ethanol de-ionized water mixture made with 9 ml of ethanol and 7 ml of de-ionized water (i.e., solution A). De-ionized water was used as the anti-solvent to precipitate DPA (i.e., solution B). The flow rates for the solutions A and B were the same at 0.15 ml/min while the oil flow rates were 0.25 ml/min. The water dilution method was used to separate the aqueous and oil phases and to prepare DPA suspension in pure de-ionized water.

The separated  $\text{BaSO}_4$  and DPA suspensions were analyzed by dynamic light scattering (DLS, 90Plus, Brookhaven Instruments Corp., Holtsville, NY) for size, size distribution and  $\zeta$ -potential measurements. The size measurements were complemented by characterization with field emission transmission electron microscopy (FEG-TEM, Model CM20, Philips, Eindhoven, The Netherlands) and field emission scanning electron microscopy (FEG-SEM, LEO 982, LEO Electron Microscopy Inc., Thornwood, NY).

### 3. Results and discussion

Fig. 2a shows a TEM image of  $\text{BaSO}_4$  nanoparticles from the first reactive crystallization experiment. The

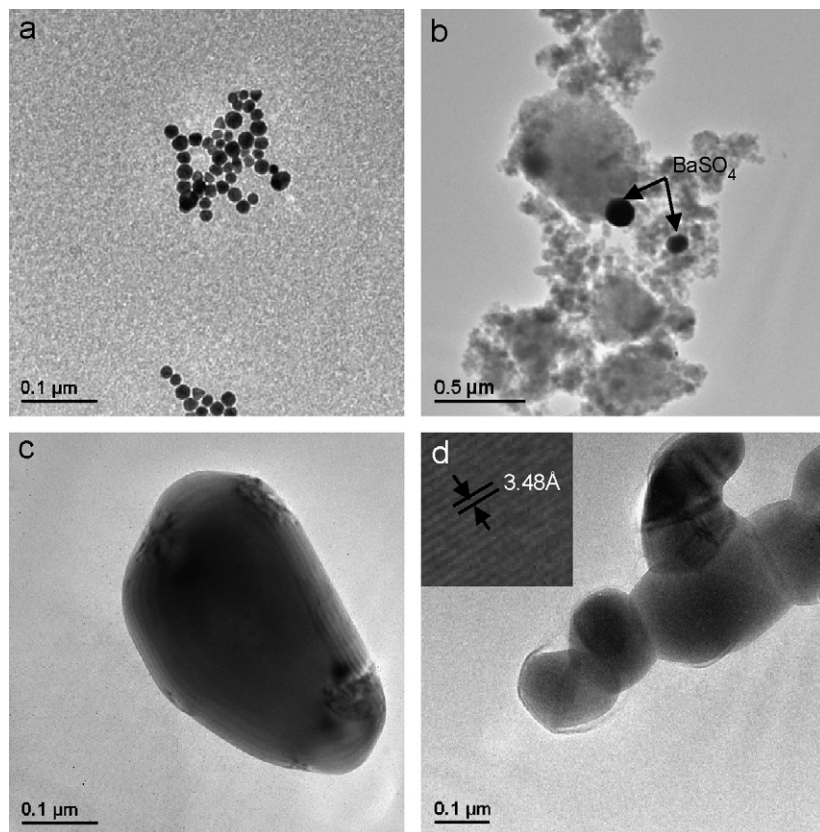


Fig. 2. Particles produced by T-junction crystallization methods: (a) TEM image of  $\text{BaSO}_4$  nanoparticles produced at 0.010 M  $\text{BaCl}_2$ ; (b) TEM image of  $\text{BaSO}_4$  nanoparticles produced at 0.015 M  $\text{BaCl}_2$ ; (c) TEM image of DPA nanoparticles; and (d) aggregated DPA nanoparticles.

Table 1  
Summary of average size, size distribution and surface charge of  $\text{Ba}_2\text{SO}_4$  and DPA nanoparticles measured by DLS and TEM

Nanoparticles	Size (nm)—TEM	Size (nm)—DLS	CV(%)—DLS	$\zeta$ -potential (mV) at pH 5.8
$\text{BaSO}_4$ @0.010 M $\text{BaCl}_2$	15	184	49	-39.7
DPA	183	213	49	-48.2

average diameter of the nanoparticles was  $\sim 15$  nm, and the particles were generally spherical. They tended to aggregate as small clusters of nanoparticles in the size range of about 100 nm. From the DLS distribution (Table 1), we measured the average size of 184 nm, which corresponded to the size of nanoparticle aggregates from the TEM image. The coefficient of variation (CV), which is defined as the ratio of standard of deviation to average particle size was about 49%. The measured  $\zeta$ -potential was  $-39.7$  mV in the de-ionized water environment. With the slight increase in the  $\text{BaCl}_2$  concentration from 0.01 to 0.015 M, the size of nanoparticles increased significantly to about 70–150 nm (Fig. 2b). Also, it appeared that the degree of dispersion of  $\text{BaSO}_4$  nanoparticles increased and the particles were well separated as shown in Fig. 2b. The  $\text{BaSO}_4$  particles are pointed by the black arrows, whereas the darker contrast background could not be determined and may be the residual materials from the unreacted precursors. The data suggested that the particle size, distribution and dispersion

are sensitive to the solution concentration. Other factors such as the water to surfactant molar ratio could also affect the  $\text{BaSO}_4$  particle size and polydispersity, as reported by Qi et al [16].

Fig. 2c shows that the average size of DPA particles was about 183 nm with a somewhat elongated shape. Some of the particles were agglomerated as indicated in Fig. 2d. The high-resolution TEM image confirmed that the particles were DPA as its  $d$ -spacing (3.48 Å) was indexed through a fast Fourier transform method. In comparison to the TEM data, the average size was measured to be about 212 nm, and the  $\zeta$ -potential is  $-48.2$  mV by DLS in the water environment as listed in Table 1.

For the DPA crystallization, it is postulated that the creation of emulsion promotes enhanced mixing, resulting in higher levels of supersaturation compared to conventional crystallization. It is generally accepted that higher levels of supersaturation in anti-solvent and cooling crystallization increases the nucleation rate relative to the

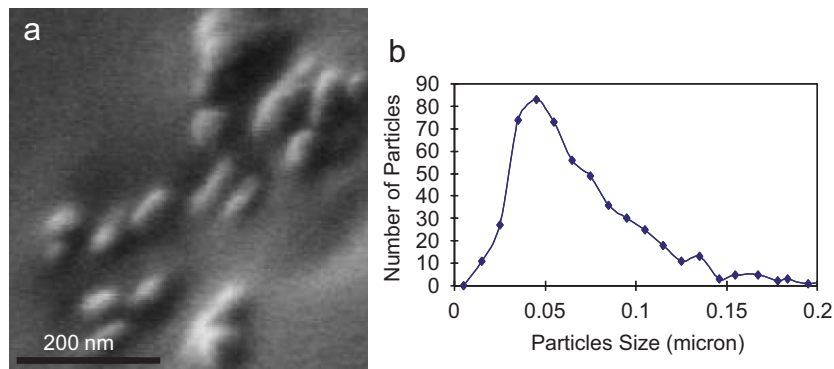


Fig. 3. Particles produced by beaker-based W/O emulsion method: (a) SEM image of BaSO<sub>4</sub> particles produced at 0.010 M BaCl<sub>2</sub> and (b) size distribution of BaSO<sub>4</sub> particles determined from SEM micrographs.

growth rate resulting in smaller size crystals. Other DPA emulsion crystallization experiments were conducted with essentially the same experimental configuration but with 800  $\mu\text{m}$  inner diameter tubes [17]. In these experiments, crystals were also in the sub-micron range. Moreover, higher flow rates resulted in smaller particles. This behavior is attributed to higher supersaturation achieved at the higher flow rates due to enhanced mixing. However, for BaSO<sub>4</sub> crystallization, larger crystals were observed at the higher BaCl<sub>2</sub> concentration along with some unidentifiable material. Other investigators have observed a maximum in crystal size with increasing BaCl<sub>2</sub> concentration [18,19]. Apparently for this reactive crystallization of ionic nature, supersaturation level alone does not directly correlate to crystal size.

BaSO<sub>4</sub> crystallization experiments were also conducted by preparing two aqueous solutions of reactants dispersed as fine droplets in vegetable oil and mixing them in a beaker. These batch experiments also resulted in nanosize range particles with a single-modal size distribution around  $\sim 70$  nm as shown in Fig. 3. The particle sizes observed from the batch experiments were not substantially different than those described here where the emulsions for the two reactant streams were formed in the T-junctions in a continuous mode.

From these results one may conclude that droplet size and hydrodynamics are not important parameters in determining the crystal size in BaSO<sub>4</sub> crystallization. Rather, it is the creation of emulsion streams of aqueous reactants with their subsequent mixing that is the predominant factor in obtaining nanosize range crystals. Nevertheless, utilization of the microreactor technology for nanoparticle processing would be in line with recent trends in crystallization technology toward semi-continuous and continuous operation in order to achieve more consistent and controllable performance.

#### 4. Conclusions

We have successfully synthesized BaSO<sub>4</sub> and 2,2'-dipyridylamine (DPA) nanoparticles in a continuous mode

by using the microfluidic-based emulsion and mixing approach as examples of reactive crystallization and anti-solvent recrystallization. The sizes of BaSO<sub>4</sub> and DPA nanoparticles were measured in the range of 15–100 and 200 nm, respectively. For both systems, as long as the emulsion-based approach was used, nanoparticles in a narrow size range were always obtained for a wide range of operating conditions including operation in the batch mode. The results here offer the possibility that the emulsion crystallization approach can be used as a new avenue for producing nanoparticles for a variety of operating conditions including utilization of the micro-reactor technology for continuous operation in order to achieve more consistent and controllable performance.

#### References

- [1] National Research Council, *Beyond the Molecular Frontier: Challenges for Chemistry and Chemical Engineering*, The National Academic Press, Washington, DC, 2003, pp. 36–40.
- [2] B. Zheng, L.S. Roach, J.D. Tice, C.J. Gerdts, D. Chen, R.F. Ismagilov, *Proceedings from the Eighth International Conference on Miniaturized Systems for Chemistry and Life Sciences*, Malmö, Sweden, September, 2004, pp. 145–147.
- [3] S.A. Khan, A. Günther, F. Traschel, M.A. Schmidt, K.F. Jensen, In: *Proceedings from the Eighth International Conference on Miniaturized Systems for Chemistry and Life Sciences*, Malmö, Sweden, September 2004, pp. 411–413.
- [4] S.A. Khan, A. Günther, M.A. Schmidt, K.F. Jensen, *Langmuir* 20 (2004) 8604–8611.
- [5] M. Joanicot, A. Ajdari, *Science* 309 (2005) 887–888.
- [6] F. Debuigne, L. Jeunieau, M. Wiame, J.B. Nagy, *Langmuir* 16 (2000) 7605–7611.
- [7] T. Thorsen, R.W. Roberts, F.H. Arnold, S.R. Quake, *Phys. Rev. Lett.* 86 (2001) 4163–4166.
- [8] J.H. Xu, S.W. Li, J. Tan, Y.J. Wang, G.S. Luo, *AIChE J.* 52 (2006) 3005–3010.
- [9] D.R. Link, S.I. Anna, D.A. Weitz, H.A. Stone, *Phys. Rev. Lett.* 92 (2004) 545031–545034.
- [10] M. Yasuno, S. Sugiura, S. Iwamoto, M. Nakajima, A. Shono, K. Satoh, *AIChE J.* 50 (2004) 3227–3233.
- [11] A.S. Utada, E. Lorenceau, D.R. Link, P.D. Kaplan, H.A. Stone, D.A. Weitz, *Science* 308 (2005) 537–541.
- [12] D.R. Lide, *CRC Handbook of Chemistry and Physics*, 86th ed., 2005–2006.

- [13] D.G. Bokern, K.A. Hunter, K.M. McGrath, *Langmuir* 19 (2003) 10019–10027.
- [14] H. Oosterhof, R.M. Geertman, G.J. Witkamp, G.M. van Rosmalen, *J. Cryst. Growth* 198/199 (1999) 754–759.
- [15] T.G. Zijlema, R.J.A.J. Hollman, G.J. Witkamp, G.M. Van Rosmalen, *J. Cryst. Growth* 198/199 (1999) 789–795.
- [16] L. Qi, J. Ma, H. Cheng, Z. Zhao, *Colloid Surf. A* 108 (1996) 117–126.
- [17] S. Kovenklioglu, et al., unpublished work, 2007.
- [18] D.L. Marchisio, A.A. Barresi, M. Garbero, *AIChE J.* 48 (2002) 2039–2050.
- [19] D.C.Y. Wong, Z. Jaworski, A.W. Nienow, *Chem. Eng. Sci.* 56 (2001) 727–734.